Symmetry of rolled-up rectangular lattice nanotubes

2006 J. Phys.: Condens. Matter 18 8139

(http://iopscience.iop.org/0953-8984/18/35/002)

INSTITUTE OF PHYSICS PUBLISHING JOURNAL OF PHYSICS: CONDENSED MATTER

J. Phys.: Condens. Matter **18** (2006) 8139–8147 doi:10.1088/0953-8984/18/35/002

Symmetry of rolled-up rectangular lattice nanotubes

Ivanka Milošević and Milan Damnjanović

Faculty of Physics, University of Belgrade, PO Box 368, 11001 Belgrade, Serbia

E-mail: ivag@afrodita.rcub.bg.ac.yu

Received 27 April 2006, in final form 3 July 2006
Published 15 August 2006
Online at stacks.iop.org/JPhysCM/18/8139

Abstract

The high symmetry of a single-wall nanotube made of a rectangular lattice sheet rolled up into a cylinder is described by a line group. Such a tube is characterized by helical symmetry, while it has translational periodicity if the squares of a rectangular lattice vector are commensurate or if its chiral vector is orthogonal to a rectangular lattice vector. Possible additional symmetry elements are consequences of the non-translational symmetries of the layer (e.g. rotational axis and mirror planes). Except for a two-fold axis, they appear only if a chiral vector matches specific, rather restrictive, conditions.

1. Introduction

The discovery of carbon nanotubes (CNTs) [1] set off extensive research of their physical properties and the synthesis of the other kinds of nanotubes (NTs) [2]. One of the generic qualities of nanotubes is their high symmetry, extensive use of which has helped not only to interpret certain experimental data but also to predict their fundamental properties [3].

Likewise a single-wall CNT, which can be described as a tube made of a single graphite layer rolled up into a cylinder, all other kinds of nanotubes can be imagined as a rolled-up layer (or concentrically rolled-up layers). The underlying lattice of the layers is, in most of the cases studied previously, hexagonal.

However, there are also nanotubular forms that are rolled up from layers with a rectangular lattice. Quite recently, the formation of single-crystal nanorings of zinc oxide by the spontaneous coaxial uniradial and epitaxial self-coiling of a polar nanobelt has been reported [4]. A polar nanobelt has a rectangular lattice [5] and the symmetry of a nanoring is actually the symmetry of a cylindrical rectangular lattice. Also, one of the types of carbon pentaheptites, which has been proved to be unstable against folding [6], has a rectangular lattice. The same lattice type has been observed in boron nets of the ternary borides $ThMoB_4$ and $YCrB_4$ [7], and predicted numerically for boron nanotubes [8]. In the case of BC_2N NTs, i.e. type II [9] which are characterized by a rectangular lattice, it is possible to switch to a hexagonal lattice (at the cost of doubling the unit cell) [10] and thus to apply the method of symmetry analysis originally developed for single-wall CNTs [12]. However, this method is

0953-8984/06/358139+09$30.00

generally not applicable to the rectangular lattices and, most likely, the above examples are just a few among many layered compounds with a rectangular lattice that can form viable tubular nanostructures. Thus, an ever-increasing number of predicted and already-synthesized forms, together with the well-known advantages of application of symmetry, motivate this effort to derive the full symmetry groups of all possible nanotubes with underlying rectangular lattices.

2. Essentials of line groups

Line groups consist of symmetries of structures that are periodic along a single direction. The periodicity of the line groups is not constricted to translational periodicity, but includes possible generalizations to regular incommensurate structures. Namely, each line group is a product $\boldsymbol{L} = \boldsymbol{Z}\boldsymbol{P}_n$ of an axial point group $\boldsymbol{P}_n$ (where n is the order of its principle axis) and an infinite cyclic group of *generalized translations* $\boldsymbol{Z}$, which may be either a screw axis $\boldsymbol{T}_Q(f)$ or a glide plane $\boldsymbol{T}_\mathrm{c}(f)$, generated by $(C_Q|f)$ (where the Koster–Seitz symbol denotes rotation by $2\pi/Q$ around the principal axis, which is conveniently chosen as the z-axis, followed by translation by f along the same axis) and $(\sigma_v|f)$, respectively.

As none of the factors is subject to crystallographic restrictions, rod groups [13] actually represent only a few special cases of the line groups: 80 out of an (uncountably) infinite number, to be precise. Thus, the principle axis n of $\boldsymbol{P}_n$ may be any positive integer and, this way, seven countably infinite families of axial point groups can be distinguished: $\boldsymbol{C}_n$, $\boldsymbol{S}_{2n}$, $\boldsymbol{C}_{nh}$, $\boldsymbol{D}_{nv}$, $\boldsymbol{C}_{nv}$, $\boldsymbol{D}_{nd}$, $\boldsymbol{D}_{nh}$. Moreover, Q may be any real number (to achieve uniqueness of C_Q, we assume $Q \geqslant 1$). Obviously, only for $Q = q/r$ rational (for r and q co-primes), $\boldsymbol{T}_Q(f) = \boldsymbol{T}_q^r(f)$ contains pure translations for fq, while the translations in the glide plane by $2f$ are always present.

It is textbook knowledge that $\boldsymbol{Z}\boldsymbol{P} \stackrel{\mathrm{def}}{=} \{zp|z \in \boldsymbol{Z},\, p \in \boldsymbol{P}\}$ is a group if and only if $\boldsymbol{Z}$ and $\boldsymbol{P}$ commute, i.e. if, for each z and p, there are z' and p' such that $zp = p'z'$. When applied to line groups, this compatibility condition gives altogether 13 different infinite families [11], some of them having several factorizations. The symmetry of incommensurate structures is described by the first and the fifth family line groups, $\boldsymbol{T}_Q(f)\boldsymbol{C}_n$ and $\boldsymbol{T}_Q(f)\boldsymbol{D}_n$, for Q irrational. All other line group families refer exclusively to translationally periodic (i.e. commensurate) systems, and have one of the following forms: $\boldsymbol{T}(f)\boldsymbol{P}_n$ (symmorphic families 2, 3, 6, 9 and 11, where $\boldsymbol{T}(f)$ is a pure translational group), $\boldsymbol{T}_{2n}^1(f)\boldsymbol{P}_n$ (zig-zag families 4, 8 and 13), and $\boldsymbol{T}_\mathrm{c}(f)\boldsymbol{P}_n$ (families 7, 10, 12 and, as alternative factorizations, 6, 8, 11 and 13).

In the context of this paper, it is important to stress that each line group $\boldsymbol{L}$ has a maximal subgroup that belongs to the first line group family $\boldsymbol{L}^{(1)}$. Such a subgroup consists of all the roto-helical transformations (combinations of the rotations around the principle axis and translations) $(C_Q|f)^t C_n^s$ of the group $\boldsymbol{L}$. The index of the subgroup $\boldsymbol{L}^{(1)}$, i.e. $|\boldsymbol{L}|/|\boldsymbol{L}^{(1)}|$, is two (four) for line groups from the families 2–8 (9–13). The remaining elements combine roto-helical transformations with vertical mirror or glide planes, horizontal mirror or roto-refractional planes, and U axes (rotation for π around the axis in the xy-plane). Obviously, $\boldsymbol{L}^{(1)} = \boldsymbol{L}$ if and only if $\boldsymbol{L}$ is a first family line group.

The presence of the non-trivial rotational factor $\boldsymbol{C}_n$ ($n > 1$) in the first family (sub)group clearly introduces non-uniqueness of the helical factor $\boldsymbol{T}_{Q'}(f)$. Namely, all the products $\boldsymbol{T}_{Q_s}(f)\boldsymbol{C}_n$ generated by C_n and $Z_s = (C_{Q'}|f)C_n^s = (C_{Q_s}|f)$ with $Q_s = Q'n/(Q's + n)$ ($s = 0, \ldots, n-1$) give the same group $\boldsymbol{L}^{(1)}$. Therefore, uniqueness can only be achieved by a convention (figure 1): let Q denote the greatest finite value among Q_s, which is (by $[x]$ and $\{x\}$, we denote integral and fractional parts of x):

$$Q = \begin{cases} Q' & \text{if } n \leqslant Q', \\ \dfrac{nQ'}{n + Q' + Q'[-\frac{n}{Q'}]} & \text{if } n \geqslant Q'. \end{cases} \qquad (1)$$

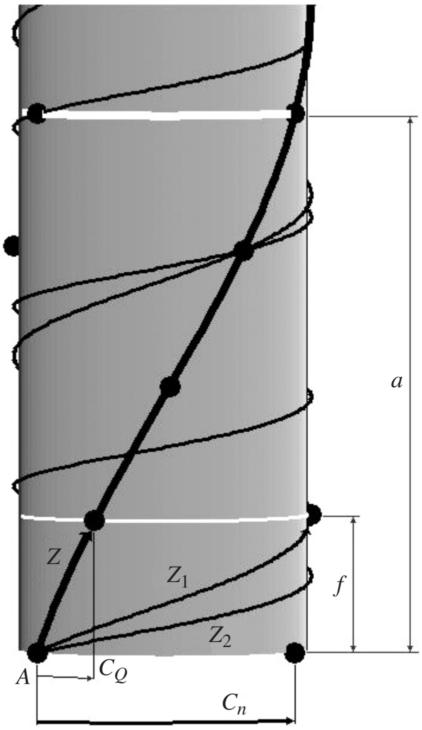

Figure 1. First family line group $\boldsymbol{T}_q^r(f)\boldsymbol{C}_n$ (for $r = 1$, $n = 3$ and $q = Q = 12$). Each atom represents a unique element of the group mapping A to this atom; generators Z and C_n are depicted by arrows. Different helices are generated by the transformations $Z_s = ZC_n^s$; the convention (1) singles out $Z_0 = Z = (C_Q|f)$ (thick helix) with the greatest slope. As the group is commensurate, its period $a = \tilde{q}f$ ($\tilde{q} = 4$) is depicted.

In particular, for the commensurate line groups, this means that, instead of $Q' = q'/r'$, we can use $Q_s = q/(r_0 + s\tilde{q})$ $(s = 0, \ldots, n-1)$, and

$$Q = \frac{q}{r}, \qquad \text{with: } q = \mathrm{LCM}(q', n) = n\tilde{q}, \qquad r = \frac{q}{n}\left\{\frac{r'n}{q'}\right\}. \tag{2}$$

Clearly, $(C_q^r|f)^t C_n^s = (C_q^{rt+s\tilde{q}}|tf)$ is, for $s = -r$ and $t = \tilde{q}$, the least pure translation; consequently, the translational period of $\boldsymbol{T}_q^r(f)\boldsymbol{C}_n$ is:

$$a = \tilde{q}f. \tag{3}$$

For example, the group combining pure translations (therefore $f = a$) $\boldsymbol{T}(a) = \boldsymbol{T}_1^0(a)$ with rotations $\boldsymbol{C}_n$ is, by this convention, $\boldsymbol{T}(a)\boldsymbol{C}_n = \boldsymbol{T}_n^1(a)\boldsymbol{C}_n$ (i.e. $r = 1$, as $r = 0$ gives infinite Q). Note that, besides the U-axis, giving the fifth family group with any roto-helical subgroup, all other symmetries are compatible only with achiral (translational and zig-zag) roto-helical groups: $\boldsymbol{L}^{(1)} = \boldsymbol{T}(a)\boldsymbol{C}_n$ (families 2, 3, 6, 7, and 9–12) and $\boldsymbol{L}^{(1)} = \boldsymbol{T}_{2n}^1(a/2)\boldsymbol{C}_n$ (families 4, 8 and 13).

3. Roto-helical transformations of a cylindrical rectangular lattice

Let us consider a two-dimensional rectangular lattice with primitive vectors $\boldsymbol{A}_1$ and $\boldsymbol{A}_2$ along the x- and y-axes, respectively. Apart from translational symmetry, there may also be other

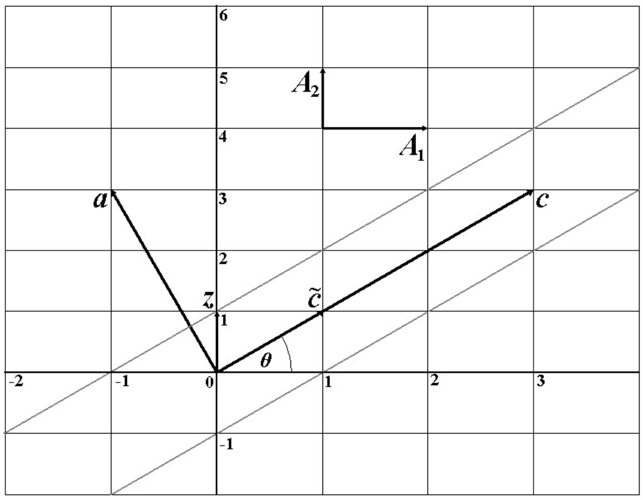

Figure 2. Rectangular layer with $A_1/A_2 = \sqrt{3}$. The chiral vector $\boldsymbol{c}$ of the nanotube (3, 3) (depicted in figure 1), together with the corresponding chiral angle $\theta = \pi/6$, reduced chiral vector $\tilde{\boldsymbol{c}} = (1, 1)$ and the grey lines containing ending points of the lattice vectors $\boldsymbol{z}_i^{\pm}$ (z_s^+ corresponds to the line group transformations Z_s, figure 1), are given. This tube is commensurate (as all tubes rolled up from this lattice, since $A_1^2/A_2^2 = 3$ is rational) with the roto-helical line group $\boldsymbol{T}_{12}^1(\frac{3}{2}A_2)\boldsymbol{C}_n$. The vectors $\boldsymbol{a} = (-1, 3)$ and $\boldsymbol{z} = (0, 1)$ correspond to the translational period and to the helical generator $(C_{12}^1|\frac{3}{2}A_2)$.

symmetries determined by the arrangement of the atoms within a unit cell. These additional symmetries are mirror and glide planes, the U-axis, and the non-trivial principle axis which is two-fold, except in the case of the square lattice ($A_1 = A_2$) where it can be of order four.

Now, let us define the *chiral vector* as $\boldsymbol{c} = (n_1, n_2) = n_1\boldsymbol{A}_1 + n_2\boldsymbol{A}_2$. It is biuniquely determined by its length c and slope, i.e. the *chiral angle* θ (figure 2):

$$c = \sqrt{n_1^2A_1^2 + n_2^2A_2^2}, \qquad \sin\theta = \frac{n_2A_2}{c}. \tag{4}$$

The nanotube (n_1, n_2) is obtained by folding the layer in a way that the chiral vector becomes a circumference of the tube. Since the tubes characterized by the chiral vectors $\boldsymbol{c}$ and $-\boldsymbol{c}$ are identical (only mutually rotated for π), it is sufficient to consider the tubes with $n_2 \geqslant 0$, i.e. $0 \leqslant \theta < \pi$. However, the tubes with equal length chiral vectors, but with the chiral angles θ and $\pi - \theta$, are enantiomers. Therefore, taking the right enantiomer only, we may restrict θ to the interval $[0, \pi/2]$. It is convenient to single out two special types of tubes: $\mathcal{X}_n = (n, 0)$ and $\mathcal{Y}_n = (0, n)$, i.e. those with chiral angles $\theta = 0$ and $\pi/2$.

The folding changes the symmetry: translations of a two-dimensional rectangular lattice become roto-helical transformations of a cylindrical web [12, 10]. To demonstrate this, we introduce the *reduced chiral vector* $\tilde{\boldsymbol{c}}$ as the minimal vector that is collinear with the chiral vector $\boldsymbol{c}$: i.e. $\tilde{\boldsymbol{c}} = \boldsymbol{c}/n = \tilde{n}_1\boldsymbol{A}_1 + \tilde{n}_2\boldsymbol{A}_2$, where

$$n = \mathrm{GCD}(n_1, n_2). \tag{5}$$

Hence, $\tilde{n}_1$ and $\tilde{n}_2$ are co-primes and translation for the reduced chiral vector $\tilde{\boldsymbol{c}}$ becomes a minimal rotation around the nanotube axis. Such n successive rotations make a full circle, showing that the nanotube's pure rotational axis is of order n, or, in other words, that $\boldsymbol{C}_n$ is the maximal rotational subgroup of the point group factor of $\boldsymbol{L}$.

Translations of the layer are generated by the reduced chiral vector $\tilde{\boldsymbol{c}}$ and any other vector $\boldsymbol{z} = z_1\boldsymbol{A}_1 + z_2\boldsymbol{A}_2$, satisfying the condition $|\tilde{\boldsymbol{c}} \times \boldsymbol{z}| = A_1A_2$. Diophantine equations

$\tilde{n}_2 z_1 - \tilde{n}_1 z_2 = \pm 1$ in $\boldsymbol{z}$ essentially underlie such a condition. Also, there are two families of solutions to the Diophantine equations:

$$\boldsymbol{z}_i^{\pm} = (z_{1i}^{\pm}, z_{2i}^{\pm}) = \mp \boldsymbol{z}_0 \pm i(\tilde{n}_1, \tilde{n}_2), \qquad \boldsymbol{z}_0 = \begin{cases} (0,1) & \text{if } \boldsymbol{c} = (n,0), \\ (-1,0) & \text{if } \boldsymbol{c} = (0,n), \\ \left(\tilde{n}_2^{\varphi(\tilde{n}_1)-1}, \dfrac{\tilde{n}_2^{\varphi(\tilde{n}_1)} - 1}{\tilde{n}_1}\right) & \text{otherwise}, \end{cases} \tag{6}$$

where $\varphi(x)$ is the Euler function giving the number of co-primes with x that are less than x. For the co-primes x and y, the Euler theorem yields $y^{\varphi(x)} = 1 + Jx$ for a uniquely defined integer $J = (y^{\varphi(x)} - 1)/x$, i.e. $x\{y^{\varphi(x)}/x\} = 1$, meaning that $y^{\varphi(x)-1}$ is the inverse of y modulo x (i.e. it is the least natural number which, when multiplied by y, has the form $1 + Jx$; thus, it can also be denoted as $y_{(x)}^{-1}$).

Obviously, the solutions are distributed on the lines (figure 2) parallel with to chiral direction $\boldsymbol{c}$ at the distance $f = A_1 A_2/\tilde{c}$, i.e.

$$f = \frac{A_1}{\sqrt{\tilde{n}_1^2 \frac{A_1^2}{A_2^2} + \tilde{n}_2^2}}. \tag{7}$$

The lattice translations $\boldsymbol{z}_i^{\pm}$ become screw axes generators $(C_Q|f)$ on the tube which, when combined with $\boldsymbol{C}_n$, give roto-helical group. (This is a manifestation of the aforementioned non-uniqueness.)

The opposite solutions, $\boldsymbol{z}_i^{+}$ and $\boldsymbol{z}_i^{-}$ ($\boldsymbol{z}_i^{+} = -\boldsymbol{z}_i^{-}$), give mutually inverse transformations on the tube, thus generating the same helical group. In order to get the helical generator with f positive, one should choose a solution $\boldsymbol{z} = \boldsymbol{z}_i^{-}$, and, to accommodate the previous convention (1), it should be the closest to the perpendicular line to $\boldsymbol{c}$, but not on it.

Evidently, f is a fractional translation of the screw axis generator. To find Q, we note that, as c is the circumference of the tube (thus corresponding to the rotation for 2π), the length of the projection of $\boldsymbol{z}$ onto $\boldsymbol{c}$ corresponds to the rotation for $2\pi/Q$. Therefore, $Q = c^2/\boldsymbol{c}\cdot\boldsymbol{z}$ and:

$$Q = n\frac{\tilde{n}_1^2 \frac{A_1^2}{A_2^2} + \tilde{n}_2^2}{\tilde{n}_1 z_1 \frac{A_1^2}{A_2^2} + \tilde{n}_2 z_2}. \tag{8}$$

Note that for $\mathcal{X}_n$ and $\mathcal{Y}_n$ we get (for $\boldsymbol{z} = \boldsymbol{z}_i^{-}$) rational number $Q = n/i$, which (after applying convention (2) for $q' = n$, and $r' = i$) gives a purely translational $\boldsymbol{Z}$ with $f = a$ (being equal to A_2 and A_1, respectively), i.e. $\boldsymbol{L}^{(1)} = \boldsymbol{T}_n^1(a)\boldsymbol{C}_n$.

Hence, the derivation of the first family subgroup of the line group of the tube (n_1, n_2) is now completed: translations of the layer are on the tube transformed into the line group

$$\boldsymbol{L}^{(1)} = \boldsymbol{T}_Q(f)\boldsymbol{C}_n, \tag{9}$$

with group parameters given by equations (5), (7) and (8). Note that f and Q/n depend only on the reduced chiral vector $\tilde{\boldsymbol{c}}$, i.e. they characterize the ray of the tubes $n(\tilde{n}_1, \tilde{n}_2)$ (being defined by the fixed co-primes $\tilde{n}_1$ and $\tilde{n}_2$).

To conclude, independently of the layer structure, the roto-helical part of the nanotube symmetry is $\boldsymbol{L}^{(1)}$, while the arrangement of the atoms within an elementary cell may give rise to the additional symmetries of the nanotubes. The latter will be analysed after a discussion on the commensurability of the tubes obtained.

4. Commensurability

Unlike the hexagonal case, rolling up a rectangular lattice may give an incommensurate structure. The commensurability condition is equivalent to the rationality of Q. Namely, as in equation (8), all the terms beside Q and A_1^2/A_2^2 are integers; Q is rational if A_1^2/A_2^2 is a rational number. Conversely, if the denominator in (8) does not vanish, A_1^2/A_2^2 may be expressed in terms of Q as $A_1^2/A_2^2 = (n\tilde{n}_1^2 - \tilde{n}_2 z_2 Q)/(\tilde{n}_1 z_1 Q - n\tilde{n}_1^2)$, showing that rationality of Q is also a necessary condition, except for tubes of the types $\mathcal{X}_n$ and $\mathcal{Y}_n$ (which are, as has already been pointed out, always commensurate). It is of practical and conceptual importance to stress that when A_1^2/A_2^2 is rational (i.e. when there are co-primes α_1 and α_2 such that $A_1^2/A_2^2 = \alpha_1/\alpha_2$) all the rolled-up tubes (n_1, n_2) are commensurate, since $Q = q'/r'$ is rational. The group parameters are easily found from the equations given in the previous section and by applying the conventions that have been introduced (2).

In the commensurate case, the translational period and helicity parameter r can be calculated directly as follows. Obviously, pure translations on the tube correspond to the two-dimensional (2D) lattice vectors which are perpendicular to the chiral vector. The minimum among such vectors is $\boldsymbol{a} = a_1\boldsymbol{A}_1 + a_2\boldsymbol{A}_2$, where a_1 and a_2 are co-primes such that the length $a = \sqrt{a_1^2 A_1^2 + a_2^2 A_2^2}$ is the tube period (3), and it satisfies the orthogonality condition $\tilde{\boldsymbol{c}} \cdot \boldsymbol{a} = \tilde{n}_1 a_1 \alpha_1 + \tilde{n}_2 a_2 \alpha_2 = 0$. These conditions give $\boldsymbol{a} = -\frac{\tilde{n}_2\alpha_2}{\alpha}\boldsymbol{A}_1 + \frac{\tilde{n}_1\alpha_1}{\alpha}\boldsymbol{A}_2$, $a = \frac{1}{\alpha}\sqrt{\tilde{n}_1^2\alpha_1^2 A_2^2 + \tilde{n}_2^2\alpha_2^2 A_1^2}$. Thus, from equations (3) and (7) one can easily find the translational period a:

$$\tilde{q} = a/f = \frac{\tilde{n}_1^2\alpha_1 + \tilde{n}_2^2\alpha_2}{\alpha}, \qquad q = n\frac{\tilde{n}_1^2\alpha_1 + \tilde{n}_2^2\alpha_2}{\alpha}, \tag{10}$$

$$a = A_2\sqrt{\frac{\alpha_1}{\alpha}\tilde{q}} = A_1\sqrt{\frac{\alpha_2}{\alpha}\tilde{q}}. \tag{11}$$

In order to find r, we note that the lattice vector $\boldsymbol{z}$, related to the screw axis generator $(C_q^r|\frac{1}{\tilde{q}}a)$, is of the form $\boldsymbol{z} = \frac{1}{\tilde{q}}\boldsymbol{a} + \frac{r}{\tilde{q}}\tilde{\boldsymbol{c}}$, where the first term corresponds to the fractional translation f along the tube, and the second term corresponds to the rotational part C_q^r. Using the previously found expression for $\boldsymbol{a}$, we get $\boldsymbol{z} = \frac{(r\tilde{n}_1 - \tilde{n}_2\frac{\alpha_2}{\alpha})a_1 + (r\tilde{n}_2 + \tilde{n}_1\frac{\alpha_1}{\alpha})a_2}{\tilde{q}}$. As $\boldsymbol{z}$ is a lattice vector, its coordinates are integers. Hence, for the first coordinate we have $r\tilde{n}_1 = \tilde{n}_2\frac{\alpha_2}{\alpha} + i\tilde{q}$. Dividing both sides by $\beta_1 = \mathrm{GCD}(\tilde{n}_1, \tilde{q})$, one gets

$$r = \frac{\tilde{n}_2\alpha_2}{\beta_1\alpha}x + i\frac{\tilde{q}}{\beta_1}, \qquad x = \left(\frac{\tilde{n}_1}{\beta_1}\right)^{-1}_{(\tilde{q}/\beta_1)} \tag{12}$$

(see the comment below equation (6)). To find i, we use the condition that the second coordinate of $\boldsymbol{z}$ is also integer: division by $\beta_2 = \mathrm{GCD}(\tilde{n}_2, \tilde{q})$ gives $r\frac{\tilde{n}_2}{\beta_2} + \tilde{n}_1\frac{\alpha_1}{\beta_2\alpha} = j\frac{\tilde{q}}{\beta_2}$; when r from (12) is substituted, it reads $\frac{\tilde{n}_2^2\alpha_2}{\alpha\beta_1\beta_2}x + i\frac{\tilde{q}}{\beta_1}\frac{\tilde{n}_2}{\beta_2} + \tilde{n}_1\frac{\alpha_1}{\beta_2\alpha} = j\frac{\tilde{q}}{\beta_2}$. According to (10) $\tilde{n}_2^2\alpha_2 = \tilde{q}\alpha - \tilde{n}_1^2\alpha_1$, we get

$$\frac{\tilde{q}\alpha}{\alpha\beta_1\beta_2}x - \frac{\tilde{n}_1\alpha_1}{\alpha\beta_2}\left(\frac{\tilde{n}_1}{\beta_1}x\right) + i\frac{\tilde{q}}{\beta_1}\frac{\tilde{n}_2}{\beta_2} + \tilde{n}_1\frac{\alpha_1}{\beta_2\alpha} = j\frac{\tilde{q}}{\beta_2}.$$

Now we substitute the bracket using the integer $X = (x\frac{\tilde{n}_1}{\beta_1} - 1)\beta_1/\tilde{q}$; after cancelations, we divide both sides by $\frac{\tilde{q}}{\beta_1\beta_2}$ to obtain the equation $i\tilde{n}_2 = (\frac{\tilde{n}_1\alpha_1}{\alpha}X - x) + j\beta_1$. Finally, using its solutions $i = (\frac{\tilde{n}_1\alpha_1}{\alpha}X - x)\tilde{n}_{2_{(\beta_1)}}^{-1} + j\beta_1$ in (12), we get the complete series:

$$r_j = r + j\tilde{q}, \qquad r = \tilde{q}\left\{\frac{\tilde{n}_2\alpha_2}{\beta_1\alpha\tilde{q}}x + \left(\frac{\tilde{n}_1\alpha_1}{\alpha}X - x\right)\frac{\tilde{n}_{2_{(\beta_1)}}^{-1}}{\beta_1}\right\}, \tag{13}$$

where r is the solution matching the conventions that have been introduced.

5. Additional symmetry elements

Besides, under the translations, the layer may be invariant under the C_2 rotations and, for the square lattice, also under the C_4 rotations. In such a case, the tubes become invariant under the horizontal two-fold axis (the U-axis) and the symmetry is described by a fifth family line group $\boldsymbol{T}_Q(f)\boldsymbol{D}_n$. Its roto-helical group is an index-two subgroup, and the U-axis is the remaining coset representative.

As emphasized at the end of the section 2, the additional symmetries may be combined only with the achiral roto-helical subgroups $\boldsymbol{T}^1_n(a)\boldsymbol{C}_n$ and $\boldsymbol{T}^1_{2n}(a/2)\boldsymbol{C}_n$ (i.e. when $\tilde{q} = 1, 2$), referring only to the commensurate tubes. In particular, we showed that $\tilde{q} = 1$ characterizes the tube types $\mathcal{X}_n$ and $\mathcal{Y}_n$ only. Thus, in the $\tilde{q} = 2$ case, none of the reduced chiral vector coordinates vanish (otherwise $\tilde{q} = 1$), implying that $\frac{\tilde{n}_1^2}{\mathrm{GCD}(\tilde{n}_1,\alpha_2)}\frac{\alpha_1}{\mathrm{GCD}(\tilde{n}_2,\alpha_1)}$ and $\frac{\tilde{n}_2^2}{\mathrm{GCD}(\tilde{n}_2,\alpha_1)}\frac{\alpha_2}{\mathrm{GCD}(\tilde{n}_1,\alpha_2)}$ in equation (10) must be equal to 1. A simple analysis shows that this is possible only if $\alpha_1 = \alpha_2 = |\tilde{n}_1| = \tilde{n}_2$, i.e. in the case of a square lattice and diagonal chiral vectors $\boldsymbol{c} = n(1, 1)$ and $\boldsymbol{c} = n(-1, 1)$.

Hence, for the achiral tubes, vertical mirror planes (glide planes) of the layer, when perpendicular to the chiral vector, give vertical mirror planes (glide planes) of the tube. When parallel to the chiral vector, the vertical mirror plane becomes the horizontal mirror plane of the tube, while the vertical glide plane becomes the roto-refractional axis S_{2n} of the tube. Therefore, in the special case of achiral tubes, the additional 2D lattice symmetries can be combined and, this way, all the line group families may be obtained, as shown in figure 3.

6. Discussion

Full symmetry of all the possible NTs with underlying rectangular lattices is found and described by the line groups. It is shown that these NTs may not have translational symmetry, in contrast to the NTs obtained by rolling up a layer with a hexagonal lattice. Translationally periodic (without helical symmetry tubes) $\mathcal{X}_n$ and $\mathcal{Y}_n$ can be obtained from any rectangular lattice, while the commensurate tubes with non-trivial helical symmetry can be obtained only if the square of the lattice period ratio is rational. In this case, the chiral angle is $\sin\theta = \tilde{n}_2\sqrt{\frac{\alpha_2}{\alpha\tilde{q}}}$. It is interesting to note that to each (of infinitely many) line groups corresponds a set of rolled-up rectangular lattice nanotubes.

Let us stress that the general results that are presented enable straightforward derivation of the symmetry (and its physical consequences) of the increasing number of reported nanotubes with rectangular lattices, such as ZnO seamless nanorings [5], carbon pentahaptite [6] and boron [8] nanotubes. Simply substituting the parameters of the lattice and the chiral indices n_1 and n_2, we get all the group parameters of the first family subgroup using the expressions presented; the possible additional symmetries of the layer are then easily included if preserved in the folded configuration.

There are various physical consequences of the line group symmetry. It automatically singles out helical quasi-momentum $\tilde{k}$ and angular momentum [14, 12] as the conserved quantum numbers of all the nanotubes; when the U-axis and mirror planes are present, there are also the corresponding parities. However, the more familiar linear quasi-momentum k is applicable only to the commensurate tubes. Thus, for incommensurate nanotubes the energy bands are given as the functions $E(\tilde{k})$ over the helical Brillouin zone $(-\pi/f, \pi/f]$, while for the commensurate tubes the usual Brillouin zone is also applicable. Analogously, straightforwardly generalizing the Bloch theorem, we conclude that the eigenstates of the

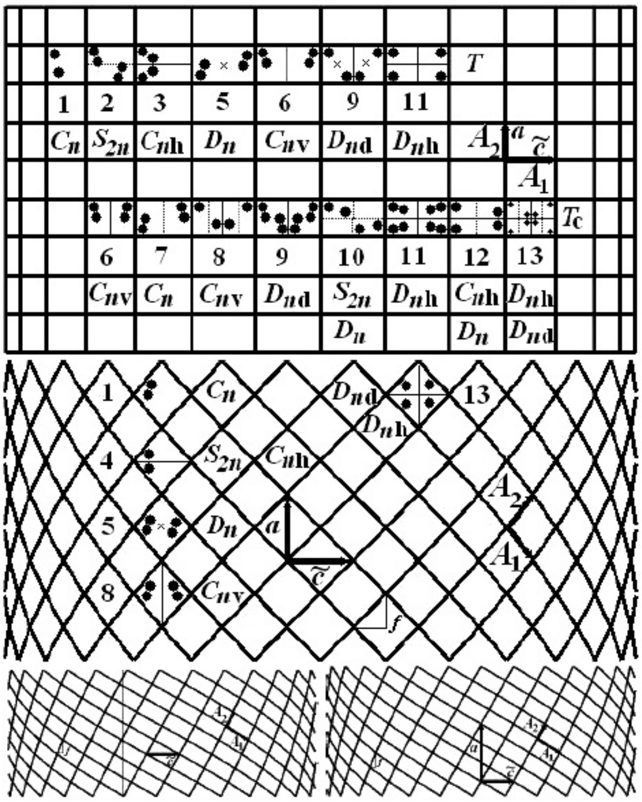

Figure 3. Top: nanotube (30, 0), being commensurate irrespective of A_1^2/A_2^2, with the first family subgroup $\boldsymbol{T}(f)\boldsymbol{C}_{30}$, $f = a = A_2$, and reduced chiral vector $\tilde{\boldsymbol{c}} = (1, 0)$. Depending on the arrangements of the atoms in the elementary cell of the layer, ten different families of line groups (given below each illustration) may be realized by combining different point factors with a purely translational group ($\boldsymbol{Z} = \boldsymbol{T}$) or glide plane group ($\boldsymbol{Z} = \boldsymbol{T}_\mathrm{c}$; dashed line). Possible additional symmetry elements are mirror planes (solid lines), roto-refractional axes (dashed line), and U-axes (crosses). Middle: nanotube (30, 30) of the square lattice layer ($A_1 = A_2$). Its first family subgroup is $\boldsymbol{T}_{60}^1(f)\boldsymbol{C}_{30}$. (It may be enlarged for some particular atomic arrangements.) Bottom: nanotubes (30, 30) folded from the layers with $A_1^2/A_2^2 = \pi^2/3 \approx 3$ and $A_1^2/A_2^2 = 3$. The corresponding line groups are $\boldsymbol{T}_{\frac{30+10\pi^2}{10+3\pi^2}}(\sqrt{\frac{3\pi^2}{3+\pi^2}})\boldsymbol{C}_{30}$ and $\boldsymbol{T}_{120}(A_1/2)\boldsymbol{C}_{30}$. In the first case (left panel), the vertical line passes solely through the origin of the bottom unit cell, emphasizing the incommensurability of the tube. As for the additional symmetry elements, the U-axis is the single possibility in both cases.

incommensurate nanotubes are characterized by the helical momentum $\tilde{k}$. One direct consequence is the appearance of the chiral (i.e. helical) currents in such nanotubes [12, 8]. The energy band degeneracies match the dimensions of the irreducible representations of the line groups, which is 1 and 2, and for commensurate groups with mirror planes this may also be 4.

Acknowledgments

This work is supported by the Serbian Ministry of Science and Environmental Protection (Project No. 141017) and the Greek–Serbian bilateral scientific project No. 451-01-02501.

References

[1] Iijima S 1991 *Nature* **354** 56
[2] Tenne R, Homyonfer M and Feldman Y 1998 *Chem. Mater.* **10** 3225
Remškar M 2004 *Adv. Mater.* **16** 1
Chopra N G, Luyken R G, Cherry K, Crespi V H, Cohen M L, Louie S G and Zettl A 1995 *Science* **269** 966
Weng-Sieh Z, Cherrey K, Chopra N G, Blase X, Miyamoto Y, Rubio A, Choen M L, Louie S G, Zettl A and Gronsky R 1995 *Phys. Rev.* B **51** 11229
Nakamura H and Matsui Y 1998 *J. Am. Chem. Soc.* **117** 2651
Hacohen Y R, Grunbaum E, Tenne R, Sloan J and Hutchison J L *Nature* **395** 337
Hu W B, Zhu Y Q, Shu W K, Chang B H, Terrons M, Grobert N, Terrons H, Hare J-P, Kroto H W and Walton D R M 2000 *Appl. Phys.* A **70** 231
Wu J, Liu S, Wu C, Chen K and Chen L 2002 *Appl. Phys. Lett.* **81** 1312
Yada M, Mihara M, Mouri S, Kuroki M and Kijima T 2002 *Adv. Mater.* **14** 309
Wang Z L 2004 *J. Phys.: Condens. Matter* **16** R829
[3] Damnjanović M, Milošević I, Dobardžić E, Vuković T and Nikolić B 2005 *Applied Physics of Nanotubes: Fundamentals of Theory, Optics and Transport Devices* ed S V Rotkin and S Subramoney (Berlin: Springer) chapter 2
[4] Kong X Y, Ding Y, Yang R and Wang Z L 2004 *Science* **303** 1348
[5] Milošević I, Stevanović V, Tronc P and Damnjanović M 2006 *J. Phys.: Condens. Matter* **18** 1939
[6] Terrones H, Terrones M, Hernández E, Grobert N, Charlier J-C and Ajayan P M 2000 *Phys. Rev. Lett.* **84** 1716
Crespi V H, Benedict L X, Cohen M L and Louie S G 1996 *Phys. Rev.* B **53** 13303
Crespi V H, Cohen M L and Rubio A 1997 *Phys. Rev. Lett.* **79** 2093
[7] Deza M, Fowler P W, Shtogrin M and Vietze K 2000 *J. Chem. Inf. Comput. Sci.* **40** 1325
[8] Kunstmann J and Quandt A 2006 *Preprint* cond-mat/0509455
[9] Miyamoto Y, Rubio A, Cohen M L and Louie S G 1994 *Phys. Rev.* B **50** 4976
[10] Damnjanović M, Vuković T, Milošević I and Nikolić B 2001 *Acta Crystallogr.* A **57** 304
[11] Milošević I and Damnjanović M 1993 *Phys. Rev.* B **47** 7805
[12] Damnjanović M, Milošević I, Vuković T and Sredanović R 1999 *J. Phys. A: Math. Gen.* **32** 4097
[13] Kopsky V and Litvin D (ed) 2003 *International Tables for Crystallography* vol E *Subperiodic Groups* (Dordrecht: Kluwer)
[14] White C T, Robertson D H and Mintmire J W 1993 *Phys. Rev.* B **47** 5485